Experimental and Numerical Analysis of a Cross-Flow Turbine

M. Sinagra[1]; V. Sammartano[2]; C. Aricò[3]; and A. Collura[4]

Abstract: An important component of the management cost of aqueducts is the energy costs. Part of these costs can be recovered by transforming some of the many existing energy dissipations into electric energy by means of economical turbines. This paper describes an experimental study that has been carried out in order to (1) test the performance of an economical cross-flow turbine that maintains high efficiency within a large range of water discharges, and (2) validate a new approximate formula relating main inlet velocity to inlet pressure. It is demonstrated that the proposed formula, on the basis of some simplifying assumptions, exactly links inlet velocity to inlet pressure with any possible geometry of the cross-flow turbine. A specific facility was designed and constructed inside the hydraulic laboratory of the Dipartimento di Ingegneria Civile, Ambientale, Aerospaziale dei Materiali (DICAM) Department of the University of Palermo to carry out the experiments. Both numerical and experimental tests were carried out for the two cases of turbine impeller with and without the internal shaft. Experimental and numerical results showed a good agreement and give an excellent validation of the proposed formula, which can be readily used for a fast and reliable design of a cross-flow turbine. **DOI: 10.1061/(ASCE)HY.1943-7900.0001061.**

Author keywords: Cross-flow turbines; Water turbines; Turbine experiments; Turbine hydraulic design; Computational fluid dynamics.

Introduction

Hydro power provides more than 97% of all the electricity generated by renewable energy sources and has some special benefits with respect to other renewable energy sources like wind, solar, and biomass (Aziz and Desai 1993; Demirbas 2007). These benefits include a lower cost of installation for equal installed nominal power, higher reliability, longer duration, and almost constant production in time.

The recent trend in worldwide energy production is to guarantee a local equilibrium between energy production and energy consumption (Zanette et al. 2010; Zia et al. 2010). This implies that microhydropower and minihydropower plants could be very advantageous even if they are located in sites where only a small amount of hydraulic power is available and standard large hydro power plants are not suitable. The practical implementation of the latter has been proven uneconomical up to now, due to the need for conventional expensive equipment such as hydraulic turbines, electrical equipment and controllers designed for large hydro power plants and not suitable for small ones (Yang et al. 2010).

[1]Post-Doctoral Researcher, Dept. Ingegneria Civile, Ambientale, Aerospaziale, dei Materiali, Univ. degli Studi di Palermo, Viale delle Scienze, 90128 Palermo, Italy. E-mail: marco.sinagra@unipa.it

[2]Post-Doctoral Researcher, Dept. Ingegneria Civile, Energia, Ambientale, e dei Materiali, Univ. Mediterranea di Reggio Calabria, Italy; Dept. Ingegneria Civile, Ambientale, Aerospaziale, dei Materiali, Univ. degli Studi di Palermo, Viale delle Scienze, 90128 Palermo, Italy (corresponding author). E-mail: vincenzo.sammartano@unipa.it

[3]Researcher, Dept. Ingegneria Civile, Ambientale, Aerospaziale, dei Materiali, Univ. degli Studi di Palermo, Viale delle Scienze, 90128 Palermo, Italy. E-mail: costanza.arico@unipa.it

[4]Professor, Istituto Nazionale di Astrofisica, Osservatorio Astronomico G. Vaiana, Piazza del Parlamento 1, 90134 Palermo, Italy. E-mail: collura@astropa.unipa.it

Note. This manuscript was submitted on July 29, 2014; approved on May 19, 2015; published online on July 16, 2015. Discussion period open until December 16, 2015; separate discussions must be submitted for individual papers. This paper is part of the ***Journal of Hydraulic Engineering***, © ASCE, ISSN 0733-9429/04015040(8)/$25.00.

An important requirement for microhyropower and minihydropower schemes is their ability to maintain high efficiency for very different discharges and net head values. Experimental studies on Turgo and Pelton turbines have been carried out to determine the effect on turbine efficiency of variations in speed ratio and jet misalignment, as well as in variations of the net head (Aziz and Desai 1993; Williams and Simpson 2009; Williamson et al. 2013). To design minihydro schemes within an economical range, various proposals are available (Chattha et al. 2010; De Andrade et al. 2010, 2011; Zanette et al. 2010; Sammartano et al. 2013). Some numerical and experimental studies have also addressed the use of pumps in the reverse mode instead of the routine turbines in order to drastically reduce the hydro plant total costs (Zia et al. 2010; Carravetta et al. 2012; Carravetta et al. 2013).

Cross-flow (CF) turbines are machines with a simple geometry, design, and construction that display very good efficiency for very different load conditions. Previous studies have addressed the optimal configuration of CF turbines by using both experimental (Khosrowpanah et al. 1988; Fiuzat and Akerkar 1989; Aziz and Desai 1993) and numerical methods (De Andrade et al. 2010, 2011; Haurissa et al. 2012; Sammartano et al. 2013; Sinagra et al. 2013). Computational fluid dynamics (CFD) analysis is very useful to estimate the velocity and the pressure fields of the CF turbine within the impeller, as well as its efficiency for different flow rate values; velocity and pressure field analysis allows evaluation of the influence on the efficiency of the turbine design parameters, such as the number of blades, the inner/outer diameter ratio, and the attack angle allowed by the structural requirements. The existence of a layer of air in the turbine can also be shown to have a very important role in improving the efficiency of the turbine (Choi et al. 2008; De Andrade et al. 2011; Sammartano et al. 2013). The optimal nozzle shape and runner blade angle can be shown to be directly related to the previous parameters (Sammartano et al. 2013).

CF turbines are usually regarded as impulse machines, so that the water flow entering the impeller behaves like a free water jet leaving the nozzle (as in Pelton or Turgo turbines). Using this approach, the velocity at the inlet of the impeller should be estimated by assuming the same velocity coefficient C_T as used in the

Torricelli formula for Pelton turbines (Mockmore and Merryfield 1949; Fiuzat and Akerkar 1991; Desai and Aziz 1994; Zia et al. 2010; Chattha et al. 2010), very close to 1. This assumption is equivalent to assuming zero relative pressure at the impeller inlet. On the other hand, several studies (Yang et al. 2010; De Andrade et al. 2011; Sammartano et al. 2013) show that the pressure at the impeller inlet is far from zero. In the study by Sinagra et al. (2013) fluid dynamic analysis showed water pressure at the inlet to be much larger than zero, leading to a C_T velocity coefficient equal to $0.75 \div 0.85$, much lower than the one used for Pelton or Turgo turbines ($C_T \approx 0.98$).

In this study, a simplified hydrodynamic approach has been used to derive a simple direct relationship between the water head at the inlet and the corresponding average velocity. The resulting formula, as well as the efficiency of the turbine prototype, designed according to the approach proposed by Sammartano et al. (2013), was tested by using a specifically designed and constructed laboratory plant. The peculiarity of the turbine prototype shown in this work is that the impeller of the turbine has no internal shaft. A second set of experimental runs have been carried out in order to verify if the internal shaft can affect turbine efficiency.

Design Procedure and Tests Description

The CF turbine prototype was designed according to the procedure described in the paper by Sammartano et al. (2013). A geometrical scheme of the turbine components is given in Fig. 1.

The theoretical approach, described in the aforementioned study, shows that maximum efficiency is obtained when the absolute tangential velocity is about twice the velocity of the reference system, such that

$$V_t = V \cdot \cos\alpha \tag{1a}$$

$$U = \omega \cdot R_1 \tag{1b}$$

$$V_t = 2 \cdot U \tag{1c}$$

where V, V_t and U = the velocity norm, the tangential velocity, and the velocity of the reference system at the impeller inlet; α = the attack angle; = the rotational velocity of the impeller; and R_1 = the outer radius of the impeller (Fig. 1). The turbine was designed assuming an attack angle α equal to 22°, which provides a good equilibrium between hydraulic efficiency and structural strains, as also suggested in the literature (Aziz and Desai 1993). The following Torricelli's equation between the impeller inlet velocity V and the net head H immediately before the turbine is adopted in the aforementioned methodology:

$$V = C_T\sqrt{2gH} \tag{2}$$

where C_T is initially close to one (almost 0.97) and accounts for the particle energy losses. As Eq. (2) assumes that the pressure along the inlet circumference was exactly zero, the design procedure was iterated several times, each time using the coefficient C_T estimated by Eq. (2) using the CFD solution of the turbine designed at the previous iteration.

In order to design a prototype of the CF turbine sought, for a given C_T value, in a first step the authors selected a few parameter values on the basis of Eqs. (1) and (2), the continuity equation, and the input Q and H data. These parameters are the outer impeller radius R_1, the angle β_1 between the blade tangent and the reference system velocity direction at the impeller inlet, the nozzle profile, and the impeller width B. In a second step other design parameters, like the blade number N_b and the R_1/R_2 ratio (Fig. 1), were selected with the help of the CFD analysis. The outer radius R_1 was estimated by using Eqs. (1) and (2), for a given rotational velocity. In the study case, the designed CF turbine with 35 blades and an attack angle equal to 22° exhibited at the design point the highest efficiency η of 86%. The impeller was designed without the rotating shaft, as suggested by the low structural strains obtained in the study case according to the CFD and subsequent structural analysis.

Most of the available studies on CF turbines (Mockmore and Merryfield 1949; Fiuzat and Akerkar 1991; Desai and Aziz 1994; Chattha et al. 2010; Zia et al. 2010) estimate the inlet velocity by means of Eq. (2), adopting a C_T coefficient close to 0.98, corresponding to zero pressure at the impeller inlet. On the other hand, CFD analysis results show that the relative pressure at the impeller inlet is positive. In the study case by Sinagra et al. (2013) the authors find a velocity coefficient C_T much lower than 0.98, falling in a range between 0.75 and 0.85. Moreover, this coefficient seems vary along with water discharge for the same machine geometry and rotational speed.

A New Velocity Formula

A more precise relationship between H and V can only be predicted if the pressure p_{in} at the impeller inlet is previously estimated. In this case, assuming a steady-state condition and neglecting energy losses inside the nozzle, this relationship is given by the Bernoulli's equation:

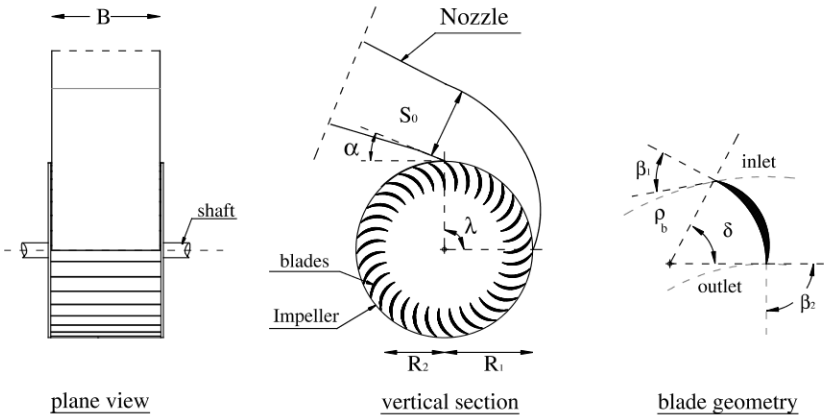

Fig. 1. Geometrical scheme of the CF turbine

J. Hydraul. Eng., 2016, 142(1): 04015040

$$H = \frac{p_{in}}{\gamma} + \frac{V^2}{2g} \tag{3}$$

where γ = the water specific weight. A rough estimation of the p_{in} pressure can be found by looking at the particle trajectory located next to the inner blade surface and passing through the center of the impeller, assuming radial symmetry and a constant norm of the relative velocity of the particle moving inside the rotating reference system, and neglecting energy losses. This particle, moving along the blade surface, will be subject to an inertial force per unit volume equal to

$$\mathbf{f} = -\rho\left(\frac{d\mathbf{V}_r}{dt} + \frac{d\mathbf{V}_a}{dt} - 2\boldsymbol{\omega} \wedge \mathbf{V}_r\right) \tag{4}$$

where $\mathbf{V}_r$ = the relative velocity of the particle; $\mathbf{V}_a$ = the velocity of the rotating reference frame at the particle location $\boldsymbol{r}$ (i.e., $\mathbf{V}_a = \boldsymbol{\omega} \wedge \boldsymbol{r}$); and $\boldsymbol{\omega}$ = a vector normal to the trajectory plane and with the norm equal to the rotational velocity ($\wedge$ is the product operator). The first and the third term on the right-hand side of Eq. (4) are normal to the blade surface and are balanced by the solid wall reaction. The second term has a radial direction and a norm equal to the centrifugal force per unit volume, given by

$$\rho\left|\frac{d\mathbf{V}_a}{dt}\right| = \rho\left|\frac{d(\boldsymbol{\omega} \wedge \boldsymbol{r})}{dt}\right| = -\rho \cdot \omega^2 r \tag{5}$$

where r = the distance of the particle from the impeller axis (the position vector $\boldsymbol{r}$ is shown in Fig. 2). The component of the force normal to the blade surface, computed according to Eq. (4), is also balanced by the solid wall reaction, but the component tangent to the same surface has to be balanced by a pressure gradient component along the relative trajectory direction. Assuming an exit angle $\beta_2 = 90°$, such that the fluid particle leaving the blade is directed toward the impeller axis, the same force acts on the particles located from the exit point of the blade up to the axis. The pressure at the inlet point of this trajectory can be computed as (Fig. 2)

$$\frac{p_{in} - p_0}{\rho} = \int_0^{R_2} \omega^2 r dr + \int_{s_1}^{s_2} \omega^2 r \cos\alpha ds = \frac{\omega^2 R_1^2}{2} \tag{6}$$

where p_0 = the relative pressure at the centre of the impeller. The same pressure increment does not apply along the part of the particle trajectory following the center of the impeller because the inlet boundary condition is given by the velocity, but the outlet boundary condition is given by the zero relative pressure. This suggests that the acceleration of the reference frame velocity affects more the norm of the relative particle velocity [along with the first term of the r.h.s. of Eq. (4)] than its pressure, and p_0 is assumed equal to zero along with the pressure gradient in this part of the trajectory.

According to the previous hypothesis, merging Eq. (6) in Eqs. (2) and (3) yields

$$V = C_V\sqrt{2g \cdot \left(H - \frac{\omega^2 R_1^2}{2g}\right)} \tag{7}$$

where C_V = the velocity coefficient, which is close to 1 only if all the previously mentioned hypotheses (steady-state conditions, radial symmetry, zero pressure at the impeller center, etc.) are exactly satisfied.

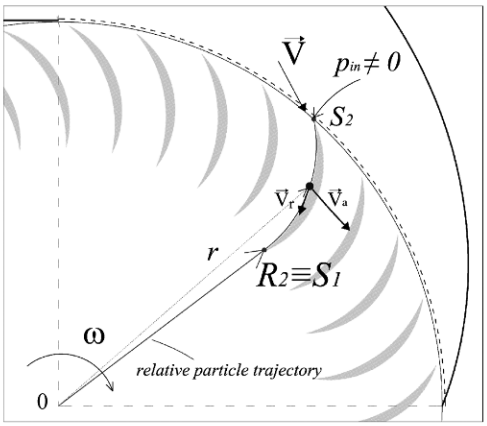

Fig. 2. Geometrical scheme of a particle moving inside the rotating reference system

Experimental Facility Overview

Experiments were carried out in the laboratory of the Department of Civil, Environmental, Aerospace, and Materials Engineering (DICAM) of the University of Palermo (Italy). The experimental facility is made up of a water-pumping system and a test stand with the CF turbine prototype coupled with a synchronous generator. Fig. 3 shows a geometrical sketch of the experimental facility.

The pumping system provides the inlet pressure and the flow rate for the CF turbine. The system operates in a closed-loop mode and is formed by an open tank reservoir, a suction pipe, a centrifugal pump, a discharge pipe, a bypass pipe, and two manual valves that allow regulation of both the flow rate and the pressure at the turbine inlet. The maximum flow rate is obtained by keeping the valve of the by-pass pipe fully closed, and the minimum pressure by keeping the valve of the discharge pipe almost closed. The

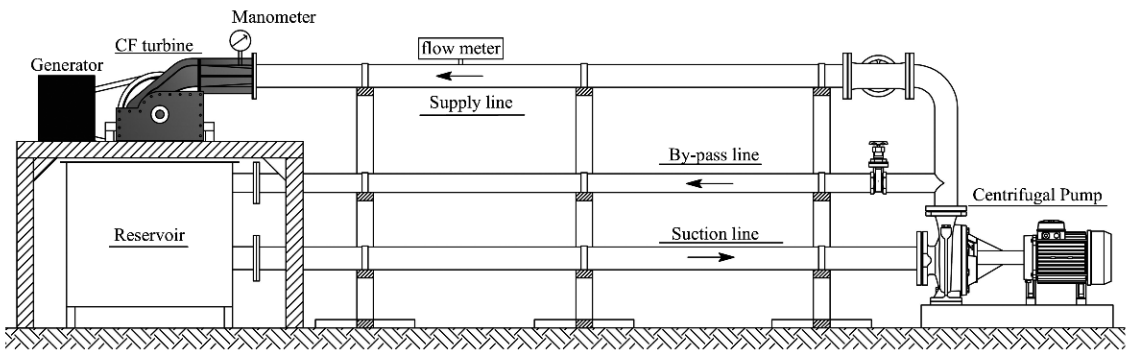

Fig. 3. Geometrical sketch of the experimental facility

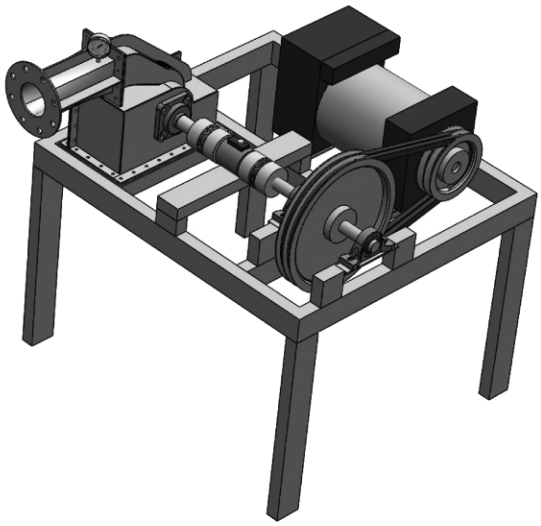

Fig. 4. Rendering of the table stand

bypass and discharge pipes are made of polyethylene, HDPE-PN 16, joined by heat fusion. The tank is used to store water and supply it to the CF turbine and has a volume of about 750 l. The suction pipeline connects the centrifugal pump to the tank, has a diameter of 150 mm and is 3.3 m long. The main features of the centrifugal pump are as follows: electric power of 15 KW, a volumetric flow rate of 60 l/s and a maximum hydraulic head of 17 m. It has the capability to work at 10 bars of pressure and is controlled by an electric panel.

The flow rate in the discharge pipe is measured by a clamp-on flow meter (Micronics, Buckinghamshire, U.K.) located in a section shortly upstream of the inlet of the CF turbine. The device is a transit-time ultrasonic flow meter designed to work with clamp-on transducers. The flow meter installed in the experimental facility allows estimation of an average velocity with 1 MHz of frequency and an accuracy of 0.5% of the reading velocity rate.

The test stand is formed by the CF turbine prototype coupled with a generator, a torque-meter and a digital manometer. The test stand is shown in Fig. 4. The CF turbine prototype, built at the laboratory of the Istituto Nazionale di Astrofisica (INAF) institute in Palermo, has the following main components: the nozzle, the impeller, and the casing. The impeller has no internal shaft and is formed by two stainless steel circular plates linked by 35 blades optimized in order to maximize the transfer of energy, according to the previously mentioned procedure. The disks are fixed to the shaft, which rotates on two bearings. The turbine case is formed by an upper sheet of metal suitably shaped by two side panels and constrained by means of bolts, which allow quick access to the inside of the machine for inspection and maintenance. The nozzle has a curved profile duct that equalizes the velocity of the water particles entering the impeller. The nozzle is welded to the turbine case and ends with a flange for connection to the penstock of the experimental plant. The holes in the stainless plates and the curved profile of the lateral sides of the nozzle were made using cutting laser technology. The blades of the impeller were modeled using the numerical control machine of the INAF laboratory. The geometry of the CF turbine was defined, as reported in the previous section, by means of numerical simulations taking into account the design strategy outlined in the previous paper by Sammartano et al. (2013). Table 1 summarizes the geometrical parameters of the previously described prototype and Fig. 5 shows the CF turbine.

At the inlet section of the nozzle, a digital manometer (Ampere S.p.A., Milano, Italy), type PM82 by Ampere, is installed. It has an accuracy of ±0.5% of the nominal full-scale reading and can measure up to 2 bars of pressure.

Table 1. Geometrical Parameters of the CF Turbine Model

Parameter	Value	Description of the geometrical parameter
D_1 (mm)	161	Impeller outer perimeter diameter
D_2 (mm)	104	Impeller inner perimeter diameter
N_b (-)	35	Number of blades
$\lambda(°)$	90	Inlet discharge angle
$\alpha(°)$	22	Angle of attack
β_1 (°)	38.9	Angle between the blade and the outer perimeter of the impeller
β_2 (°)	90.0	Angle between the blade and the inner perimeter of the impeller
ρ_b (mm)	29.8	Radius of blade
δ (°)	62.6	Central angle of blade
S_0 (mm)	47	Nozzle initial height
B (mm)	93	Nozzle width

The turbine is coupled to a synchronous generator by means of two trapezoid transmission belts with a gear ratio equal to 0.5. The generator has a horizontal axis and four rotor poles, so that with a 50 Hz frequency, it has a rotational speed of 1,500 rpm. The generator is connected to halogen lamps and is fed by direct current (DC) by means of a regulated power supply that converts the alternating current (AC) into a constant DC; this power supply system makes it possible to change the torque at the shaft end and hence its rotational velocity.

A torque-meter, which allows one to measure the torque (up to 200 Nm) transmitted from the turbine shaft to the generator shaft, is installed between the turbine and the synchronous generator. The torque-meter also makes it possible to measure the rotational velocity of the turbine shaft (up to 10,000 rpm). The torque sensor (Kistler, Winterthur, Switzerland), type 4,520 A by Kistler, has a frequency response of 1.5 KHz and an accuracy of ±0.5% of the nominal full-scale reading. The torque sensor is connected to the shaft by two coupling metal bellows. This flexible coupling allows a compensation angle between the linked shafts. The electric load, connected to the generator, is made up of 18 halogen lamps of 400 watts each, with six lamps for each phase; each phase is monitored with a voltmeter and an ampere-meter (Schneider Electric, Stezzano, Italy).

Acquisition of experimental data is controlled by a supervisory control and data acquisition (SCADA) system. The system installed in the experimental facility is a CompactLogix 5370 L3 Controller (Rockwell Automation S.r.l., Milan, Italy). The model installed in the control panel, processor 1769-L30ER by Allen Bradley (Rockwell Automation S.r.l., Milan, Italy), has a programmable logic controller (PLC) with a secure digital (SD) card for nonvolatile memory storage, network connections (USB and Ethernet/IP network), as well as two I/O compact modules (for 8 analog signals and for 16 digital signals), and a two-channel encoder. The PLC configured and designed using the software *RS-Logix 5000* (Scott 2013). The software enables real-time access to all the sensors. A *Labview* (Bishop 2010) code was developed to process and store the time series of the water discharge flowing into the turbine, the pressure at the inlet, the torque at the impeller shaft, and the rotational speed of the impeller.

Experimental Runs

As discussed in the previous section, tests were carried out mainly for validation of the efficiency curve and of the relationship in Eq. (7) between inlet head and velocity, as computed with the CFD simulations. Other tests were carried out in order to study the effect of an internal shaft on turbine efficiency. To this aim, using the same

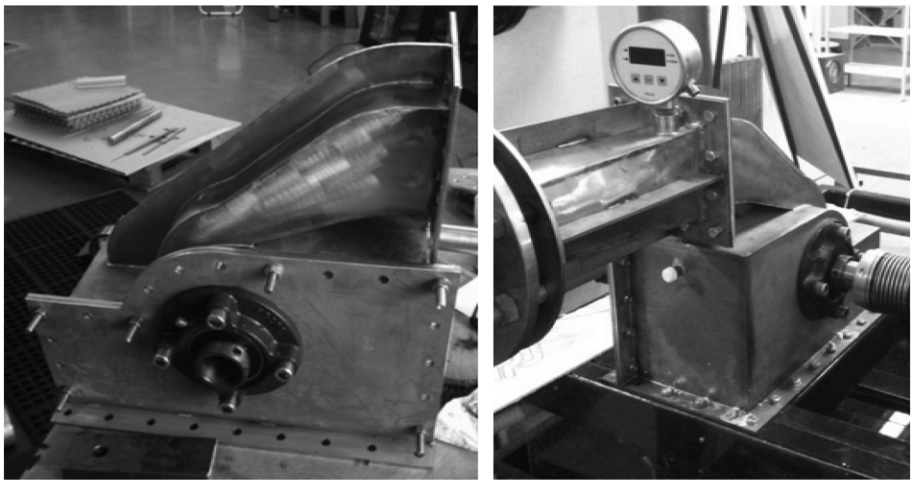

Fig. 5. Two different views of the cross-flow turbine prototype

impeller with 35 blades, two different configurations of the rotating shaft were compared: (1) without the rotating shaft, and (2) with a 30-mm-diameter shaft. For each configuration of the impeller, several series of tests were carried out, keeping a constant value of the pressure p_{up} at the nozzle inlet section (in the range 0.3–0.7 bar) and exploring a wide range of rotating velocities, from 300 to 850 rpm. For each test, the time series of the water discharge Q flowing into the turbine, the pressure at the nozzle inlet p_{up}, the torque T of the impeller shaft, and the rotational speed of the impeller were recorded. The data collected were used to estimate the velocity V_{in} and the total net head H at the nozzle inlet, the corresponding hydraulic power P_h, and the mechanical power P_m at the impeller shaft. The turbine efficiency η is evaluated as the ratio between the mechanical power P_m and the hydraulic power P_h:

$$\eta(t) = \frac{P_m(t)}{P_h(t)} \tag{8}$$

while the velocity coefficient C_V was evaluated using Eq. (7) for a given head and rotational velocity.

The time series of the aforementioned variables were filtered in order to reduce the noise of the signal and to remove the outlier values without losing the signal shape. First the data were denoised with a cubic smoothing spline; a frequency analysis of the smoothed signal by means of the Fast Fourier Transform (FFT) algorithm (Frigo and Johnson 1998) was then used for result validation. The FFT algorithm was applied to the acquired signals $f(t)$. The square of the norm ($|\text{FFT}|^2$), normalized with respect to its maximum value ($\max|\text{FFT}|^2$) was plotted versus the signal frequency. In Fig. 6, the FFT analysis of the discharge signal $Q(t)$, for a velocity ratio $V_t/U = 1.8$, is shown. The plot shows that the cubic smoothing spline of the original signal is useful for removing the noise from the signal itself.

The outlier observations were removed by using the whitening test of the residuals $r(t)$ between the original signal $f(t)$ and the smoothed one $f_s(t)$. Thus the autocorrelation of the residuals $\rho(r,k)$ was estimated in order to identify the data falling into a confidence interval of 95% coverage (Brockwell and Davis 1991):

$$\rho(r,k) = \frac{1.96}{\sqrt{N_k}}, \quad \forall\ k > 1 \tag{9}$$

where k = the adopted lag-time.

In order to estimate the error of the experimental efficiency, the standard error of the sample mean for the acquired signals, SE_f, has been estimated by the sample estimate of the population standard deviation (sample standard deviation denoted by σ_f)divided by the square root of the sample size (assuming statistical independence of the values in the sample, denoted by n_f) (Everitt 2003):

$$\text{SE}_f = \frac{\sigma_f}{\sqrt{n_f}} \tag{10}$$

Finally, after the statistical analysis was carried out on the collected data series, the time-averaged values of the velocity coefficient C_V and of the turbine efficiency were estimated by means of Eqs. (7) and (8).

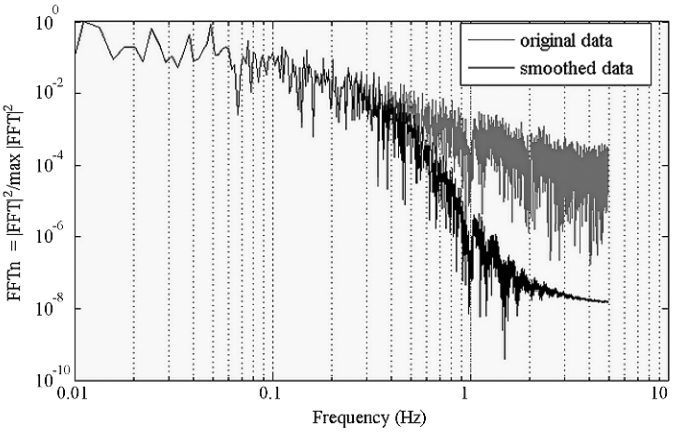

Fig. 6. Normalized power of two FFT norms (FFT_n) of the discharge signal $Q(t)$, for a velocity ratio $Vt/U = 1.8$

Results of the Experimental and the Numerical Analysis

The power P_m measured at the shaft of the turbine is a function of the machine geometry and material, as well as of both the discharge Q and the head H at the inlet of the nozzle. On the other hand, dimensionless efficiency η and velocity coefficient C_V should only be a function of the velocity ratio V_t/U, due to the geometric, kinematic, and dynamic similarity between experiments with the same velocity ratio (Ramos 2000; Seppo 2012). Experimental tests were carried out in the range of $V_t/U = 1.2$–2.2 and an inlet nozzle

pressure p_{up} in the range of 0.3–0.7 bar. Experimental results were compared with 2D numerical simulations carried out by means of the commercial solver *ANSYS* CFX. The computational domain was divided in two physical subdomains: the rotor (impeller), and the stator, which is made by the nozzle and the casing of the turbine. In the numerical simulations, both water and air phases were modeled according to the free-surface homogeneous model, where the two species share the same dynamic fields of pressure, velocity, and turbulence (*ANSYS*).

Computational domain was discretized by a single 3D layer divided in tetrahedral and prismatic elements. The prismatic discretization was created by using the Pre Inflation algorithm (*ANSYS*); this enabled capture of the strong gradients of the physical/cinematic flow variables close to the blade surface by using prismatic elements with very small extensions in the direction normal to the surface. The quality of each mesh was verified by using a preprocessing procedure by *ANSYS* ICEM CFD (*ANSYS*).The total number of discretization elements was of about 800,000: 664,000 in the rotor domain and 136,000 in the stator domain. The $k-\varepsilon$ turbulence model has been selected in the *ANSYS* CFX code among the available ones. The $k-\varepsilon$ model is very reliable, widely used, and validated with applications ranging from industrial to environmental flows, even if it has been shown to perform poorly in the boundary layers when adverse pressure gradients occur (Wilcox 1998).

The boundary conditions selected in the simulations are: (1) at the nozzle inlet water volume fraction equal to one and all assigned velocity components, and (2) at the outlet section of the casing zero relative pressure, as well as assigned velocity direction (normal to the section) and open boundary for water and air. Open boundary means that both positive and negative fluxes are allowed for water and air.

In the case of an impeller without a rotational shaft, the efficiencies were almost the same for a constant value of the relative velocity, in agreement with the aforementioned similarity laws, and the experimental efficiency was always greater than the one calculated by means of CFD analysis. This latter observation is consistent with the results of Sammartano et al. (2013) and is likely due to some numerical diffusion, as well as to the hypothesis adopted in *ANSYS* CFX about the air/water interaction (*ANSYS*). In Fig. 7, the efficiency of the turbine, estimated in each experimental run and in each numerical simulation, is plotted versus the velocity ratio V_t/U. The plot shows that the turbine attains the maximum efficiency $\eta = 82.1\%$, for a velocity ratio close to 2 ($V_t/U = 1.8$), in agreement with the aforementioned design procedure and with Eq. (1).

In Fig. 8 the velocity coefficient C_V evaluated by means of Eq. (7), from recorded experimental data as well as numerical simulations, is plotted against the velocity ratio. The regression lines of both the experimental and simulated data sets provide an excellent validation of Eq. (7), with a C_V coefficient bounded between the 0.95 and 1.0 values and only weakly affected by the actual velocity ratio. The linear regression of the estimated velocity coefficient is represented by an almost horizontal line, even though some spreading occurs; the coefficients of regression are $R^2 = 0.083$ for the experimental values and $R^2 = 0.065$ for the numerical simulations.

A second series of tests were performed in order to measure the reduction of the efficiency given by an internal impeller shaft. In these runs, a false shaft crossing the impeller was put inside the empty external shaft. The experiments were carried out with a constant inlet nozzle pressure $p_{up} = 0.4$ bar, investigating the same range of velocity ratios adopted for the first set of tests. The efficiencies versus the velocity ratio of these tests have been plotted in Fig. 9, where each point is associated to the corresponding standard

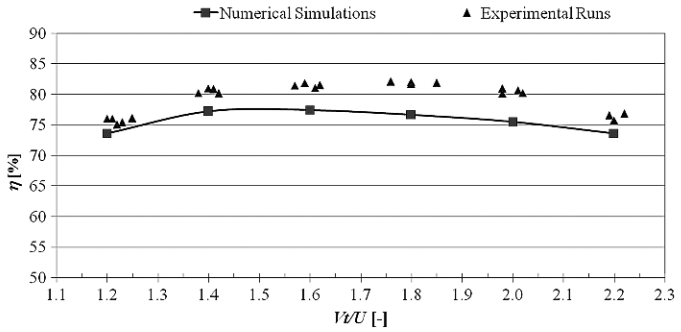

Fig. 7. Plot of the efficiency versus the velocity ratio V_t/U; comparison between the experimental and numerical results

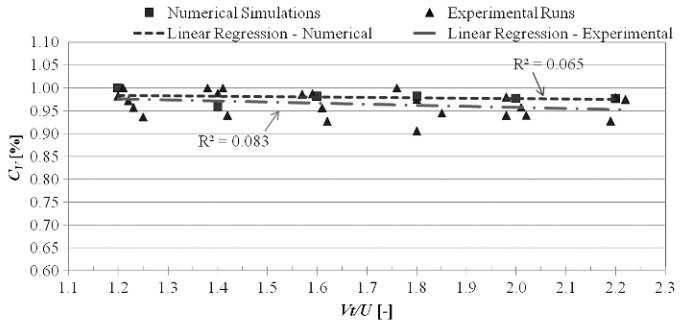

Fig. 8. Plot of the coefficient C_V versus the velocity ratio; comparison between experimental and numerical results

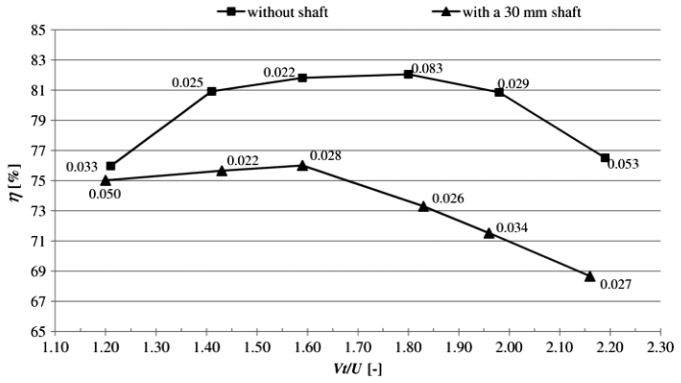

Fig. 9. Comparison of the efficiencies estimated experimentally between the prototype with and without a rotational shaft

error SE_f estimated by Eq. (10). The efficiencies of the two impeller configurations are compared with data relative to the same pressure condition ($p_{up} = 0.4$ bar). The plot shows that the trend of the efficiency curves is quite similar, but the performances of the impeller with the rotational shaft are lower than that of the impeller without a shaft, in agreement with the numerical results shown by Sammartano et al. (2013). This behavior is evident in the range of velocity ratios between 1.5 and 2.2; for lower ratios, the difference between the efficiency of the impeller with and without the shaft is negligible (75.0 and 75.6% respectively for $Vt/U = 1.2$).The velocity coefficient estimated for both configurations, with and without a shaft, are compared in Fig. 10. The plot shows that the C_V coefficient is almost constant for different values of the velocity ratio and it always attains values close to one, but is slightly smaller in the case of an impeller with a shaft.

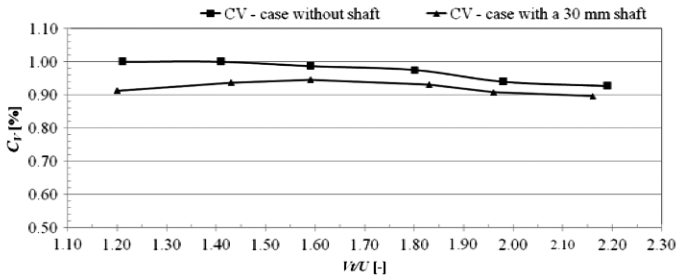

Fig. 10. Comparison of the estimated C_V between the prototype with and without a rotational shaft

The strong reduction in turbine efficiency observed for higher velocity ratios should be related to the energy dissipation occurring to the water jet before leaving the impeller. Numerical simulations were performed in order to investigate the shape of the water jet inside the rotating impeller with the internal shaft, for two different values of velocity ratio, $V_t/U = 1.2$ and $V_t/U = 1.8$. The contour plot of the water volume fraction for the velocity ratios considered is reported in Fig. 11. The plots highlight the fact that the effect of the internal shaft is different in the two cases: for a velocity ratio $V_t/U = 1.2$, the water jet inside the impeller hits the internal shaft but it keeps its main direction; for a velocity ratio $V_t/U = 1.8$, the water jet hits the shaft but also deviates from the radial direction. This implies a reduction in the energy exchanged with the impeller during the jet exit.

The shape of the water jet observed by means of the numerical simulations is confirmed by the visual observations of the outlet water jet taken during the tests. The pictures reported in Fig. 12 highlight the fact that for lower values of V_t/U (from 1.2 to 1.5), the water jet at the outlet of the turbine is inclined with respect to the vertical direction; for higher values of the relative velocity V_t/U greater than 1.5, the water jet is almost vertical.

Conclusions

The results of this experimental study can be summarized as follows:

- Experimental efficiencies in general show good agreement with their numerical estimation, computed by means of the CFD analysis; the trend is the same, but the experimental results are always slightly higher than the numerical ones.
- Laboratory tests confirmed that the maximum efficiency, 82%, is reached with a velocity ratio slightly lower than 2, in agreement with previous studies.
- The velocity coefficient C_V, estimated by means of Eq. (7), is close to 1 for all the experimental runs and independent from the velocity ratio. This means that by evaluating the inlet velocity using Eq. (7), it is possible to perform a good design of the turbine geometry, without iterating the same design according to

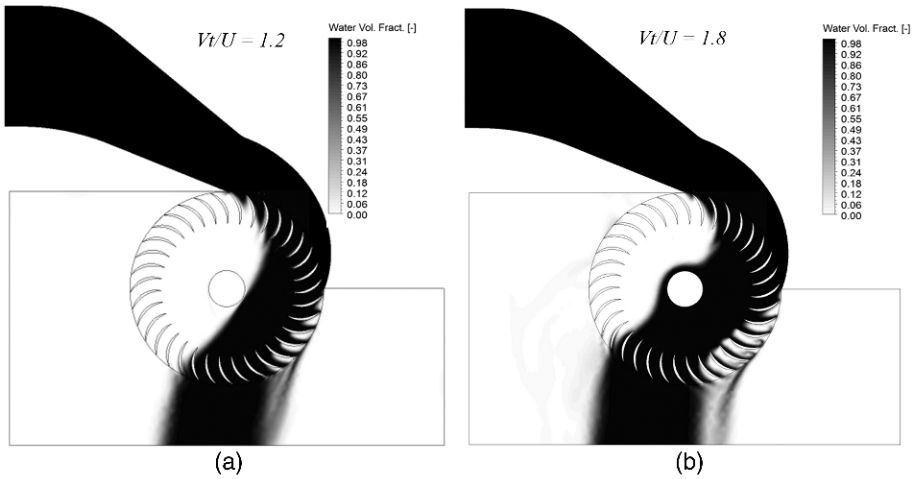

Fig. 11. Contour plots of the water volume fraction for the prototype with the internal shaft: (a) for $V_t/U = 1.2$; (b) for $V_t/U = 1.8$

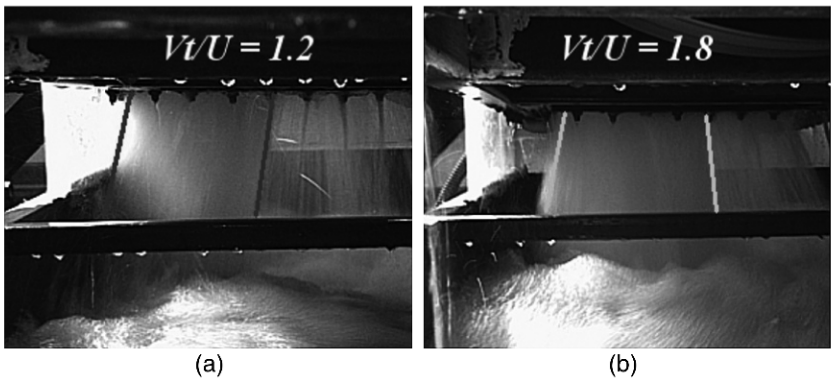

Fig. 12. Outlet water jet for the impeller with a 30-mm rotational shaft: (a) for $V_t/U = 1.2$; (b) for $V_t/U = 1.8$

the actual relationship occurring between inlet velocity V and head H.

- The impeller shaft provides a significant reduction inturbine efficiency: for a velocity ratio close to the optimal value ($V_t/U = 1.8–2.0$), the impeller with a shaft has 5% lower efficiency than the impeller without shaft. The efficiency curves tend to assume the same value for the two cases by reducing the velocity ratio (the efficiency is about 75% for a velocity ratio V_t/U close to 1.2).

Acknowledgments

Many thanks go to the technician at the hydraulic laboratory of the Department of Civil, Environmental, Aerospace, of Materials Engineering of Palermo University, Mr. M. Mannino, and to the INAF technicians, Mr. G. Di Cicca and Mr. S. Varisco, who built the impeller, the nozzle and, the case of the prototype, and also assembled the turbine. The research was supported by Hydroenergy project, PO FESR 2007-2013, Sicily and by the PRIN 2010/11 national research program.

References

ANSYS [Computer software]. Canonsburg, PA, Ansys.

Aziz, N. M., and Desai, V. R. (1993). "A laboratory study to improve the efficiency of cross-flow turbines." *Eng. Rep.*, Dept. of Civil Engineering, Clemson Univ., Clemson, SC.

Bishop, R. H. (2010). "Learning with Labview 2009." Upper Saddle River, NJ.

Brockwell, P. J., and Davis, R. A. (1991). *Time series: Theory and methods*, Springer, New York.

Carravetta, A., del Giudice, G., Fecarotta, O., and Ramos, H. M. (2013). "PAT design strategy for energy recovery in water distribution networks by electrical regulation." *Energies*, 6(1), 411–424.

Carravetta, A., Del Giudice, G., Fecarotta, O., and Ramos, H. M. (2012). "Energy production in water distribution networks: A PAT design strategy." *Water Resour. Manage.*, 26(13), 3947–3959.

Chattha, J. A., Khan, M. S., Wasif, S. T., Ghani, O. A., Zia, M. O., and Hamid, Z. (2010). "Design of a cross flow turbine for a micro-hydro power application." *ASME 2010 Power Conf.*, ASME, New York, 637–644.

Choi, Y. D., Lim, J. L., Kim, Y. T., and Lee, Y. H. (2008). "Performance and internal flow characteristics of a cross-flow hydro turbine by the shapes of nozzle and runner blade." *J. Fluid Sci. Technol.*, 3(3), 398–409.

De Andrade, J., Curiel, C., Kenyery, F., Aguillón, O., Vásquez, A., and Asuaje, M. (2010). "Numerical investigation of the internal flow in a Banki Turbine. Comparison with experimental results." *Proc., 13th Int. Symp. on Transport Phenomena and Dynamics of Rotating Machinery 2010, ISROMAC-13*, Curran Associates Inc., NY, 117–126.

De Andrade, J., Curiel, C., Kenyery, F., Aguillón, O., Vásquez, A., and Asuaje, M. (2011). "Numerical investigation of the internal flow in a Banki turbine." *Int. J. Rotating Mach.*, 12.

Demirbas, A. (2007). "Focus on the world: Status and future of hydropower." *Energy Sources Part B*, 2(3), 237–242.

Desai, V. R., and Aziz, N. M. (1994). "An experimental investigation of cross-flow turbine efficiency." *J. Fluid Eng.*, 116(3), 545–550.

Everitt, B. S. (2003). *The Cambridge dictionary of statistics*, Cambridge University Press, Cambridge, U.K.

Fiuzat, A. A., and Akerkar, B. P. (1989). "The use of interior guide tube in cross flow turbines." *Proc., Int. Conf. on Hydropower (WATERPOWER '89)*, Vol. 2, 1111–1119.

Fiuzat, A. A., and Akerkar, B. P. (1991). "Power outputs of 2 stages of cross-flow turbine." *J. Energy Eng.*, 10.1061/(ASCE)0733-9402(1991)117:2(57), 57–70.

Frigo, M., and Johnson, S. G. (1998). "FFTW: An adaptive software architecture for the FFT." *Proc., 1998 IEEE Int. Conf. on Acoustics, Speech and Signal Processing, 1998*, Institute of Electrical and Electronic Engineers Signal Processing Society (IEEE SPS), NJ, 1381–1384.

Haurissa, J., Wahyudi, S., Irawan, Y. S., and Soenoko, R. (2012). "The cross flow turbine behavior towards the turbine rotation quality, efficiency, and generated power." *J. Appl. Sci. Res.*, 8(1), 448–453.

Khosrowpanah, S., Fiuzat, A. A., and Albertson, M. L. (1988). "Experimental study of cross-flow turbine." *J. Hydraul. Eng.*, 10.1061/(ASCE)0733-9429(1988)114:3(299), 299–314.

Mockmore, C. A., and Merryfield, F. (1949). "The Banki water turbine." *Bull. Series n. 25*, Engineering Experiment Station, Corvallis, OR.

Ramos, H. (2000). "Guidelines for design of small hydropower plants." CEHIDRO, WREAN, and DED, Belfast, North Ireland.

Sammartano, V., Arico, C., Carravetta, A., Fecarotta, O., and Tucciarelli, T. (2013). "Banki-Michell optimal design by computational fluid dynamics testing and hydrodynamic analysis." *Energies*, 6(5), 2362–2385.

Scott, A.. (2013). "Instant PLC programming with RS-Logix 5000". Birmingham, United Kingdom.

Seppo, A. K. (2012). *Principles of turbomachinery*, Wiley, Hoboken, NJ.

Sinagra, M., Sammartano, V., Aricò, C., Collura, A., and Tucciarelli, T. (2013). "Cross-flow turbine design for variable operating conditions." *Procedia Eng.*, 70, 1539–1548.

Wilcox, D. C. (1998). *Turbulence modeling for CFD*, 2nd Ed., DCW Industries, Anaheim, CA, 162–165.

Williams, A. A., and Simpson, R. (2009). "Pico hydro—Reducing technical risks for rural electrification." *Renewable Energy*, 34(8), 1986–1991.

Williamson, S. J., Stark, B. H., and Booker, J. D. (2013). "Performance of a low-head pico-hydro Turgo turbine." *Appl. Energy*, 102, 1114–1126.

Yang, X., Song, Y., Wang, G., and Wang, W. (2010). "A comprehensive review on the development of sustainable energy strategy and implementation in China." *IEEE Trans. Sustainable Energy*, 1(2), 57–65.

Zanette, J., Imbault, D., and Tourabi, A. (2010). "A design methodology for cross flow water turbines." *Renewable Energy*, 35(5), 997–1009.

Zia, O., Ghani, O. A., Wasif, S. T., and Hamid, Z. (2010). "Design, fabrication and installation of a micro-hydro power plant." *Rep*.